NMR of a Synthetic Peptide Spanning the Triphosphate Binding Site of Adenosine 5′-Triphosphate in Actin†

Julian A. Barden*
Muscle Research Unit, Department of Anatomy, The University of Sydney, Sydney, N.S.W. 2006, Australia
Bruce E. Kemp
Department of Medicine, The University of Melbourne, Repatriation General Hospital, West Heidelberg, Vic. 3081, Australia
Received August 7, 1986; Revised Manuscript Received October 17, 1986

ABSTRACT: The amino acid residues 114–118 in actin were found to be implicated strongly in the binding of nucleotide, and as would be expected for such an important binding site, they are located in a completely conserved region of the actin sequence. A 19-residue peptide with the actin sequence 106–124 was synthesized in order to span the putative triphosphate binding site. Proton NMR spectra of the actin peptide 114–118 in the presence and absence of ATP indicated that Arg-116 and Lys-118 are particularly involved in binding ATP. A strong binding of ATP to the peptide 106–124 also was measured. Tripolyphosphate bound to the peptide 106–124 somewhat more weakly than ATP. Binding involved residues 115–118 and 121–124, indicating the presence of a reverse turn between these segments. Proton resonances were assigned by using two-dimensional double quantum correlated spectroscopy, one-dimensional spin decoupling techniques, one-dimensional nuclear Overhauser enhancement difference spectroscopy, and pH titration. The αCH resonances of Ala-3 and Asn-6 are markedly shifted downfield with respect to values in small unstructured peptides due to their close proximity to the side chains of Pro-4 and Pro-7, respectively. Several other resonances display chemical shifts which are indicative of a structured environment. Assignment of the amide proton resonances in H_2O and measurements of the coupling constant $^3J_{HNCH}$ and the chemical shifts of the amide protons reveal that much of the synthetic peptide, particularly the backbone, exhibits a highly structured environment and represents a good model for the triphosphate binding site in actin.

Actin monomers require a bound nucleotide, normally ATP, to maintain their structural integrity (Asakura, 1961). An X-ray diffraction analysis of actin–DNase I cocrystals (Kabsch et al., 1985) has revealed that actin consists of a smaller N-terminal domain and a larger C-terminal domain separated by a cleft. The triphosphate moiety of the bound ATP has been localized at the base of the cleft. Distances have been determined between the nucleotide site and other loci on actin by using fluorescent resonance energy transfer spectroscopy. These include 3.9 nm to Cys-10 (Miki et al., 1986), 2.1 nm to Tyr-69 (Barden & Miki, 1986), and 3.1 nm to Cys-374 (Miki & Wahl, 1984; dos Remedios & Cooke, 1984). Although the precise region involved in binding the nucleotide has not been established, residues 69–373 have been shown to bind ATP with similar affinity to intact actin although the high-affinity metal binding site is lost (Jacobson & Rosenbusch, 1976).

Phalloidin has been cross-linked to Glu-117, to Met-119, and to a lesser extent Met-355 (Vandekerckhove et al., 1985). An ATP analogue, 8-azido-ATP, has been cross-linked to Trp-356 (Hegyi et al., 1985). On this basis, the phalloidin and nucleotide binding sites on actin appear as if they may be close. That they are actually overlapped was shown by measuring nucleotide exchange in actin in the presence of phalloidin and from the determination of the maximum distance separating them (Barden et al., 1986). Moreover, this recent study showed that the actin peptide 114–118, containing Glu-117 and adjacent to Met-119, appeared to be directly implicated in binding ATP since it was extracted from an actin digest as a complex with ATP. The residues 114–118 are located in the center of a completely conserved region of the actin sequence stretching from residues 104 to 128 (Vandekerckhove & Weber, 1984). Thus, a peptide was synthesized to include as much of this region of the actin sequence as considered necessary and practical to provide a sufficiently large domain for an investigation of its interaction with ATP and tripolyphosphate.

Materials and Methods

Separation of ATP Binding Actin Pentapeptide. The pentapeptide consisting of residues 114–118 (Ala-Asn-Arg-Glu-Lys) in the actin sequence was separated from a tryptic digest in a complex with ATP as described previously (Barden et al., 1986).

Synthesis and Purification of Actin Peptide 106–124. The actin peptide 106–124 was synthesized by using the solid-phase synthesis procedure (Hodges & Merrifield, 1975) on an Applied Biosystems 430A peptide synthesizer using standard conditions as recommended by the manufacturer. Amino acid derivatives protected with the *tert*-butyloxycarbonyl group in the α-amino position and benzhydrylamine resin were obtained from the Protein Research Foundation (Osaka, Japan). The Ala, Phe, Gln, Ile, Leu, Met, and Pro side chains did not require additional protection. However, the Asp, Glu, and Thr side chains were blocked with the benzyl group, the Lys side chains were blocked with the chlorobenzyl group, and the Arg side chain was blocked with the tosyl group. The assembled peptide was simultaneously deprotected and cleaved from the resin with anhydrous HF containing 10% (v/v) anisole (Stewart & Young, 1966). Synthetic peptide was extracted with acetic acid (30% v/v) and chromatographed on SP-Sephadex as described previously (Kemp, 1979). The peptide required further purification using reverse-phase high-per-

† This work has been supported by grants from the National Health and Medical Research Council of Australia.

0006-2960/87/0426-1471$01.50/0

formance liquid chromatography (HPLC) on a Vydac preparative HPLC column (218TP, 10 μm, 2.5 × 22 cm). The column was eluted isocratically with 26% (v/v) CH_3CN in 0.1% trifluoroacetic acid. The peptide was recovered by rotary evaporation and repeated lyophilization from H_2O. The resultant peptide was pure by analytical reverse-phase HPLC on a Brownlee RP-300 aquapore column.

Amino acid analyses of the HPLC-purified peptide were in good accordance with the theoretical values. A sample concentration of 3.2 mM was used with 12.8-nmol aliquots injected. The average of two runs yielded Asx (1.94), Thr (2.04), Glx (3.00), Pro (2.04), Ala (1.49), Met (1.93), Ile (0.99), Leu (1.00), Phe (1.08), Lys (2.01), and Arg (1.00). Integration problems were presumably responsible for the low Ala yield. NMR data clearly revealed two Ala βCH_3 resonances and two Ala αCH resonances.

Proton NMR Spectroscopy. The majority of resonance assignments were obtained from NMR spectra obtained from samples in which the NH groups were exchanged. This was accomplished by initially lyophilizing the peptide in 99.8% D_2O and then in 100% D_2O. Those measurements which included the NH resonances were obtained by lyophilizing the peptide from pure H_2O. Sample pH was adjusted with NaOD or DCl and measured with an Activon BJ51130 thin-stem NMR microelectrode and a Radiometer pHM-64 meter. Values reported are meter readings uncorrected for the deuterium isotope effect. The concentration of the synthetic actin peptide 106–124 was maintained below 3.0 mM for either one-dimensional (1-D) or two-dimensional (2-D) NMR measurements. Evidence of line broadening and amide proton chemical shift changes was obtained at peptide concentrations of 4.0 mM and above in the pH range 2.5–6.5. Solubility outside this range of pH was progressively reduced. All samples were prepared in 5-mm precision tubes.

NMR spectra were recorded at 298 K at 400 MHz in the Fourier transform mode with quadrature detection using a Varian XL-400 spectrometer. The 1-D spectra were collected by using a 90° radio-frequency pulse of 13–14 μs. A spectral width of 4–5 kHz was employed with a preacquisition delay of 2.0 s. The acquisition time was 1.5 s, and generally 512–1024 scans were collected.

Non-amide resonance assignments were obtained by using double quantum filtered correlated spectroscopy (DQCOSY) (Piantini et al., 1982; Rance et al., 1983; Shaka et al., 1983).

The two-pulse scheme $90°-t_1-90°$ was followed by the reconversion pulse:

$$90°(\phi)-t_1-90°(\phi + \psi)-90°(\psi)-\text{acquisition}$$

where the radio-frequency phase ϕ is cycled through the values $\phi = k\pi/2$ for $k = 0$, 1, 2, and 3.

To ensure quadrature detection in ω_1, the phase cycle was performed for values of the receiver reference phase $\psi = 0$ and $\pi/2$. The resulting signals were alternatively added and subtracted. Spectra were acquired by dual quadrature detection and consisted of 2048 × 2048 data points obtained from 512 individual experiments. The spectra are absolute-value mode and were usually transformed without any sine bell apodization along t_1 and t_2. Accumulation of 96 free induction decays per experiment, together with a 2.0-s preacquisition delay, resulted in a total acquisition time of 24 h. The 2-D spectra were folded or symmetrized by the standard Varian software procedures.

Some assignments had to be checked by using 1-D spin decoupling procedures. The low peptide concentrations used precluded the use of 2-D techniques for the assignment of NH resonances. Following assignment of the αCH resonances, all the NH resonances were assigned by using a two-level 1-D spin decoupling procedure. The solvent resonance was irradiated with homodecoupling continuously throughout a 2.0-s preacquisition and a 1.0-s acquisition period while a low-level decoupling pulse was applied during the acquisition period to selected αCH resonances. The coupled NH resonance was then observed to collapse to a singlet.

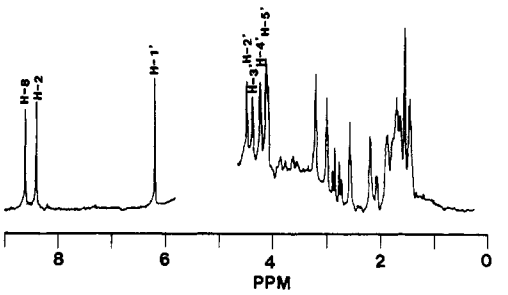

FIGURE 1: Proton NMR spectrum (pH 4.0) of the ATP-bound peptide 114–118 (ANREK) coextracted from a digest of actin. The ATP proton resonances are labeled. The ribose protons H-2′ to H-5′ obscure the αCH peptide resonances. Note the overlap between the Arg γCH_2 and the Lys βCH_2 and γCH_2 resonances. These are more mobile and shift back upfield in the ATP-free peptide shown in Figure 2.

One-dimensional nuclear Overhauser effect difference (NOED) spectra were obtained with a preacquisition delay of 2.0 s and a saturation time of 4.0 s by the method of Jones et al. (1978). The residual solvent resonance was irradiated simultaneously by using a two-level pulse scheme. All chemical shifts were referenced to internal (trimethylsilyl)propanesulfonic acid (TSS).

RESULTS

Interaction of Actin Peptide 114–118 with ATP. The tryptic peptide 114–118 consisting of the sequence Ala-Asn-Arg-Glu-Lys (ANREK) interacts strongly with ATP and is eluted in reverse-phase HPLC in a buffer of CH_3CN and 0.1% trifluoroacetic acid as described previously (Barden et al., 1986). Titration of ATP with the peptide ANREK at a peptide concentration of 0.1 mM revealed equimolar binding using the reverse-phase HPLC column. The ATP–peptide complex eluted 30 s in advance of the free peptide. A proton NMR spectrum of the complex is shown in Figure 1 with the ATP proton resonances labeled. The dissociated peptide reveals a different conformation as evidenced by the chemical shift differences. A spectrum of the free peptide is shown in Figure 2. The major differences are in the Arg γCH_2 which undergoes a downfield shift of 0.06 ppm and the Lys δCH_2 which is downfield shifted by 0.035 ppm in the presence of equimolar ATP. The Arg β and δ resonances and the Lys β, γ, and ϵ resonances undergo smaller downfield shifts.

Interaction of ATP with the Synthetic Actin Peptide 106–124. The interaction of ATP with residues 114–118 and the knowledge that phalloidin cross-links to Glu-117 (Vandekerckhove et al., 1985) and that phalloidin and the nucleotide overlap (Barden et al., 1986) together led to the peptide consisting of the actin sequence 106–124 being synthesized. The peptide sequence is Thr-Glu-Ala-Pro-Leu-Asn-Pro-Lys-Ala-Asn-Arg-Glu-Lys-Met-Thr-Gln-Ile-Met-Phe (TEAPLNPKANREKMTQIMF), and it represents an attempt to incorporate as much of the entirely conserved environment surrounding the peptide ANREK as considered manageable.

A 1-D spectrum of a 3.0 mM solution of the peptide in D_2O at 298 K and pH 3.0 is shown in Figure 3. ATP was titrated into the peptide solution over the pH range 3–6. The immediate result was that the peptide progressively precipitated.

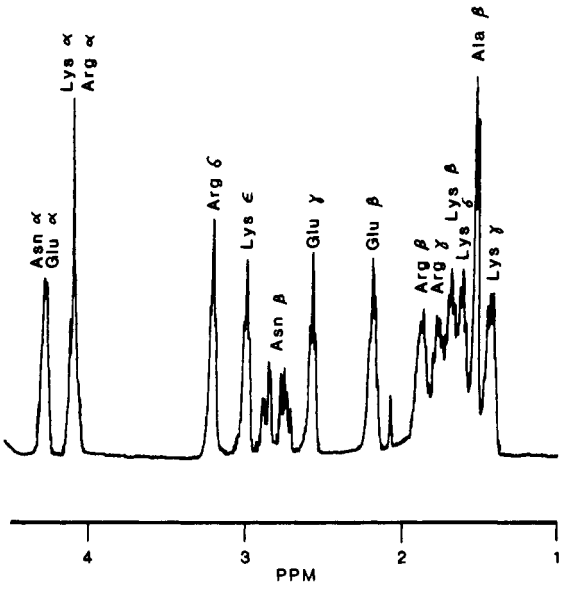

FIGURE 2: Proton NMR spectrum of the ATP-free peptide ANREK which shows an increased mobility in the Arg and Lys resonances following removal of the ATP. Residual solvent obscures the Asn αCH resonance at 4.682 ppm.

Examination of the NMR spectra revealed that the reduction in the proton resonance heights was in direct proportion to the ATP:peptide ratio. Moreover, no ATP protons were observed to resonate in the spectrum until the ATP concentration exceeded the peptide concentration. Thus, ATP binding to the synthetic peptide caused precipitation of the complex. NMR analysis of the peptide was then considered worthwhile since ATP clearly bound.

ATP binds to actin via the triphosphate side chain (Barden et al., 1980) with the β- and γ-phosphates forming the tightest bonds (Cozzone et al., 1974; Brauer & Sykes, 1981). Thus, the interaction of the peptide with tripolyphosphate was observed. The affinity was found to be much lower than the affinity of ATP although the result was the same; i.e., the peptide progressively precipitated. However, considerable line broadening was observed even at low tripolyphosphate:peptide ratios. At higher ratios (about equimolar), precipitation was observed. At intermediate ratios (0.1–0.3), evidence of binding was obtained. Selective broadening of several of the resonances was observed. Figure 4 shows a 1-D spectrum of a 3.0 mM solution of the peptide at pH 5.0 in the absence (upper) and presence (lower) of 1.0 mM tripolyphosphate at 298 K. The tripolyphosphate is in much faster exchange than ATP, and consequently, a proportionally larger effect on the peptide resonances is observed than with ATP which is in a slower exchange induced by tighter binding. The line broadening is increased with an elevation in sample temperature as the exchange rate increases. At 35 °C, most of the resonances are broadened.

Proton Resonance Assignments. Assignments of the chemical shifts, δ, were obtained by examining the correlations in DQCOSY spectra at pH 3.0 and 5.0, by 1-D spin decoupling techniques, by 1-D NOED spectra, and by pH titrations. Table I contains the values of the chemical shifts at pH 5.0 together with the values obtained from tetrapeptides by Bundi and Wüthrich (1979).

The synthetic peptide 106–124 contains 19 residues composed of 12 different amino acids which thus require assignment to individual residue number as well as to residue type. Many spin systems can be assigned unequivocally by reference to the correlations shown in Figure 5 obtained at pH 3.0 and 298 K. These include the correlation patterns of Ala, Ile, Lys, Leu, Pro, Arg, and Thr. Expanded views of a DQCOSY spectrum at pH 5.0 are shown in Figure 6 to illustrate examples of the correlation patterns.

Phe and Asn are residues which have ABX/BM spin systems in D_2O. These too are readily identifiable in Figures 3 and 5, and they are shown in the expanded contours in Figure

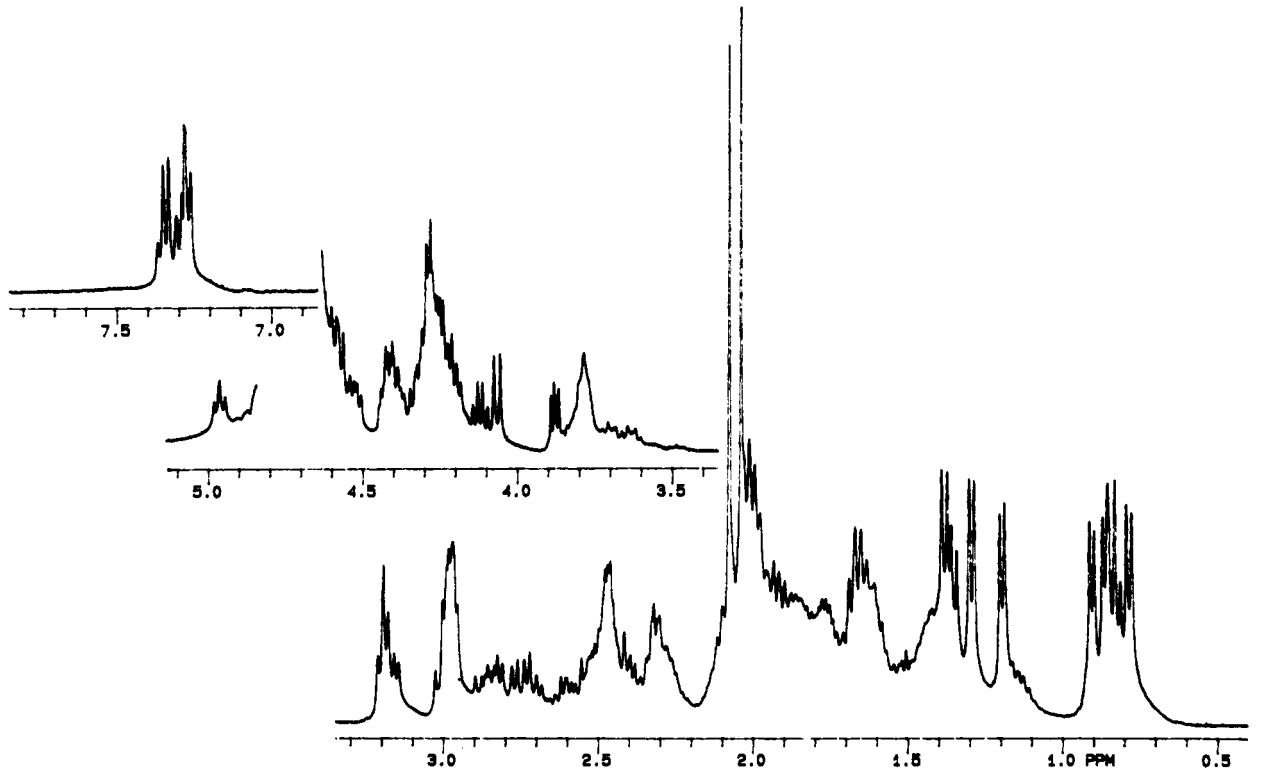

FIGURE 3: Proton NMR spectrum of the synthetic peptide 106–124 at pH 3.0, 298 K and 3.0 mM in D_2O. The peptide has the sequence TEAPLNPKANREKMTQIMF.

Table I: Chemical Shifts of Assigned Resonances in Actin Peptide 106–124 at 298 K and pH 5.0 Together with Values Expected from Unstructured Tetrapeptides from Bundi and Wüthrich (1979)

residue	no.	α	β_1	β_2	γ_1	γ_2	δ_1	δ_2	ϵ	other
Ala	3	4.588	1.373							
	9	4.264	1.403							
	GGAA	4.349	1.395							
Glu	2	4.337	2.005	1.939	2.285	2.285				
	12	4.225	1.927	1.932	2.285	2.285				
	GGEA	4.295	2.092	1.969	2.314	2.283				
Phe	19	4.595	3.173	3.035			7.290	7.290	7.360	7.360
	GGFA	4.663	3.223	2.991			7.339	7.339	7.339	7.339
Ile	17	4.085	1.788		1.444	1.159	0.806			0.844
	GGIA	4.224	1.894		1.478	1.190	0.885			0.943
Lys	8	4.302	1.814	1.860	1.460	1.403	1.663	1.663	2.992	
	13	4.302	1.814	1.860	1.460	1.403	1.663	1.663	3.003	
	GGKA	4.358	1.747	1.870	1.471	1.471	1.708	1.708	3.023	
Leu	5	4.270	1.641	1.641	1.641		0.884	0.927		
	GGLA	4.385	1.649	1.649	1.649		0.899	0.943		
Met	14	4.524	2.136	2.034	2.626	2.626			2.097	
	18	4.524	2.136	2.034	2.626	2.626			2.059	
	GGMA	4.513	2.164	2.000	2.633	2.633			2.128	
Asn	6	4.983	2.842	2.738						
	10	4.687	2.829	2.774						
	GGNA	4.755	2.831	2.755						
Pro	4	4.415	2.296	1.868	2.032	2.032	3.715	3.803		
	7	4.634	2.041	1.886	2.032	2.032	3.652	3.803		
	GGPA	4.471	2.295	1.981	2.030	2.030	3.653	3.653		
Gln	16	4.431	1.921	1.921	2.438	2.438				
	GGQA	4.373	2.131	2.010	2.379	2.379				
Arg	11	4.375	1.849	1.807	1.625	1.625	3.213	3.213		
	GGRA	4.396	1.915	1.796	1.719	1.719	3.312	3.312		
Thr	1	3.883	4.135		1.316					
	15	4.291	4.224		1.217					
	GGTA	4.346	4.220		1.232					

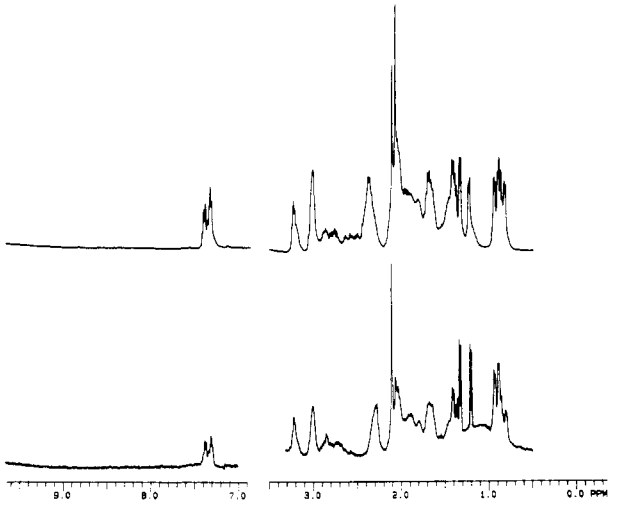

FIGURE 4: Proton NMR spectrum of the peptide 106–124 at pH 5.0, 298 K, and 3.0 mM in D_2O in the absence (upper) and presence (lower) of 1.0 mM tripolyphosphate. Significant exchange broadening occurs in the residues Asn-10, Arg-11, Lys-13, and the C-terminal four residues Gln-16 to Phe-19 as the complex is formed.

6. The βCH_2 resonances of Phe are found at 3.035 and 3.173 ppm while those of the Asn residues are found at 2.738 and 2.842 ppm and at 2.774 and 2.829 ppm, respectively, at pH 5.0. These three sets of values are comparable to those observed in small peptides (see Table I).

The pair of Glu residues and the single Gln were more difficult to assign especially since there is a pair of Met residues to further complicate the analysis. A pH titration was performed to identify the Glu γCH_2 and βCH_2 resonances. At pH 3.0, the Gln residue exhibits an identifiably unambiguous set of γCH_2 resonances. Thus, only the Met resonances remained to be identified in this region. The ϵCH_3 resonances are the sharp singlets at 2.059 and 2.097 ppm (see Figure 3), somewhat upfield of the expected position in small peptides. However, the remainder of the Met spin systems was found to be closely equivalent to the resonance positions in small peptides and individually indistinguishable (Table I). Thr-15 and one Met residue were unaffected by the binding of tripolyphosphate (Figure 4). However, the other Met residue, the Ile, and the Phe were affected. Consequently, the resonance at 2.059 ppm is assigned to Met-18, and the resonance at 2.097 ppm is assigned to Met-14.

Following identification of all the resonances in the spectrum with respect to residue type, it remained to assign them to individual residues. Thus, as unique residue types, Leu-5, Arg-11, Gln-16, Ile-17, and Phe-19 are completely assigned. This leaves two Ala, two Glu, two Lys, two Asn, two Pro, and two Thr residues to be assigned.

(*1*) *Alanine.* Ala-3 and Ala-9 have clearly distinguishable spin systems. The δ of the αCH resonances shows a particularly large difference with one resonance at 4.264 ppm, somewhat upfield of the position in small peptides (4.349 ppm), and the other resonance at 4.588 ppm, well downfield of the unstructured position. The βCH_3 resonances do not exhibit such large shifts but are clearly not overlapped, with positions centered at 1.403 and 1.373 ppm, respectively. Pro-4, which is adjacent to Ala-3, is almost certainly responsible for the large ring-induced downfield shift in the Ala αCH (Grathwohl & Wüthrich, 1976a,b). Thus, Ala-3 α and β resonances are at 4.588 and 1.373 ppm while Ala-9 resonances are at 4.264 and 1.403 ppm, respectively. Moreover, the peptide ANREK shows that Ala βCH_3 resonates at 1.521 ppm and the αCH at 4.263 ppm, similar to the values in the larger peptide. To verify this assignment, 1-D NOED specra were employed to detect the connectivities between the αCH of Ala-3 at 4.588 ppm and a Pro δ in the region 3.6–3.8 ppm. Two resonances were detected at 3.803 ppm and nearby at 3.715 ppm, thus further confirming the assignment.

(*2*) *Glutamic Acid.* Glu-2 and Glu-12 exhibit an identical pK_a of 4.20. The γCH_2 resonances are overlapped completely

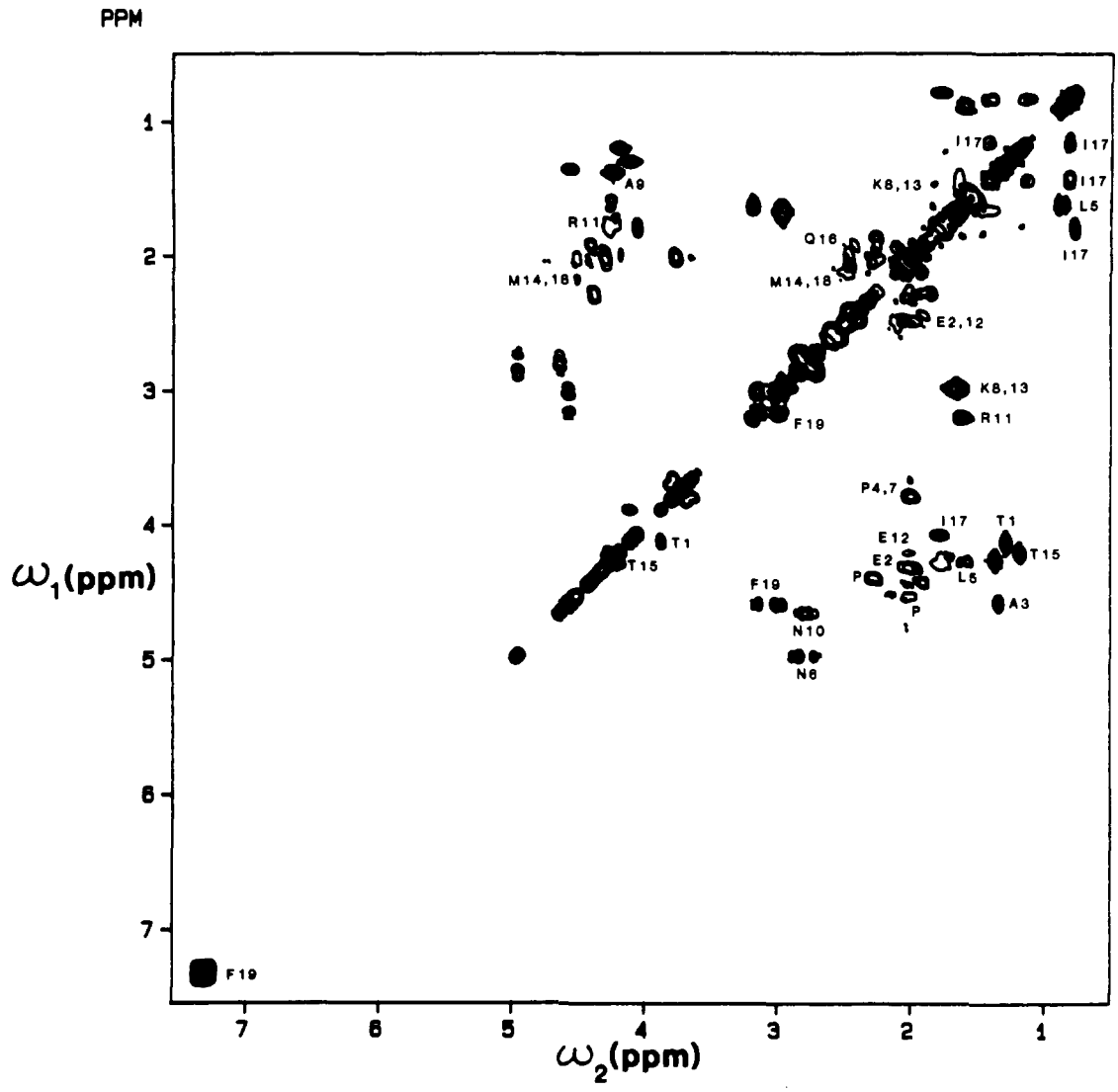

FIGURE 5: Two-dimensional double quantum correlated spectrum (DQCOSY) at pH 3.0, 298 K, and 3.0 mM in D_2O. The peaks along the diagonal can be identified by reference to the one-dimensional spectrum in Figure 3.

at 2.285 ppm. Perusal of the DQCOSY spectrum in Figure 5 and pH titrations showed that the βCH_2 resonances are not overlapped. One set of resonances are at 1.977 and 1.932 ppm while a second set resonates at 2.005 and 1.939 ppm. The corresponding αCH positions were measured from the correlations at pH 5.0. They are 4.225 and 4.337 ppm, respectively. With the exception of one αCH resonance, all the Glu resonances are upfield of their positions in small unstructured peptides (Table I). In the isolated peptide ANREK, the Glu αCH resonates at 4.15 ppm, also well upfield of its position in unstructured peptides. This suggests that the αCH resonance at 4.225 ppm is due to Glu-12 with the corresponding βCH_2 resonances at 1.977 and 1.932 ppm. Thus, the αCH of Glu-2 is assigned the position at 4.337 ppm with the corresponding βCH_2 resonances at 2.005 and 1.939 ppm. These assignments were confirmed by using 1-D NOED spectra. Following identification of the αCH of Thr-1 at 3.883 ppm and assignment of the Glu NH resonances (see later sections), a connectivity was detected by irradiating the αCH of Thr-1 and observing the coupling to the NH of Glu-2 at 8.310 ppm in H_2O.

(*3*) *Lysine.* Lys-8 and Lys-13 are essentially completely overlapped. A minor exception is the ϵCH_2 resonances, the δ of which are 2.992 and 3.003 ppm. The negligible differences in δ suggest that the environments of Lys-8 and Lys-113 are very similar. Their assignments are based on the effect on the ϵCH_2 resonances of the binding of tripolyphosphate (see Discussion).

(*4*) *Asparagine.* The pair of Asn residues displays spin systems which are readily separated by using the DQCOSY spectra in Figures 5 and 6. The βCH_2 resonances possess chemical shifts very close to those in small unstructured peptides, namely, 2.842 and 2.738 ppm and 2.829 and 2.774 ppm. However, like the Ala αCH resonances, the Asn αCH resonances are widely separated. In small peptides, the αCH is 4.755 ppm, but from Figure 6, it is clear that one Asn αCH is shifted upfield to 4.687 ppm, the same value as measured in the peptide ANREK, while the second is shifted downfield to 4.983 ppm. The latter is thus expected to be Asn-6 and is clearly the result of a ring-induced shift from the adjacent Pro-7 (Grathwohl & Wüthrich, 1976a,b). This assignment was confirmed by detecting a connectivity between the αCH of Asn-6 at 4.983 ppm and a Pro δ in the region 3.6–3.8 ppm. Such a coupling was found at 3.652 and at 3.803 ppm.

(*5*) *Threonine.* The two Thr residues are easily separated by their completely disparate spin systems. They correspond to the N-terminal Thr-1 and to Thr-15. The γCH_3 in small peptides resonates at 1.232 ppm, a value close to that of one of the Thr residues in the peptide (1.217 ppm). The corresponding βCH resonates at 4.224 ppm, similarly close to the

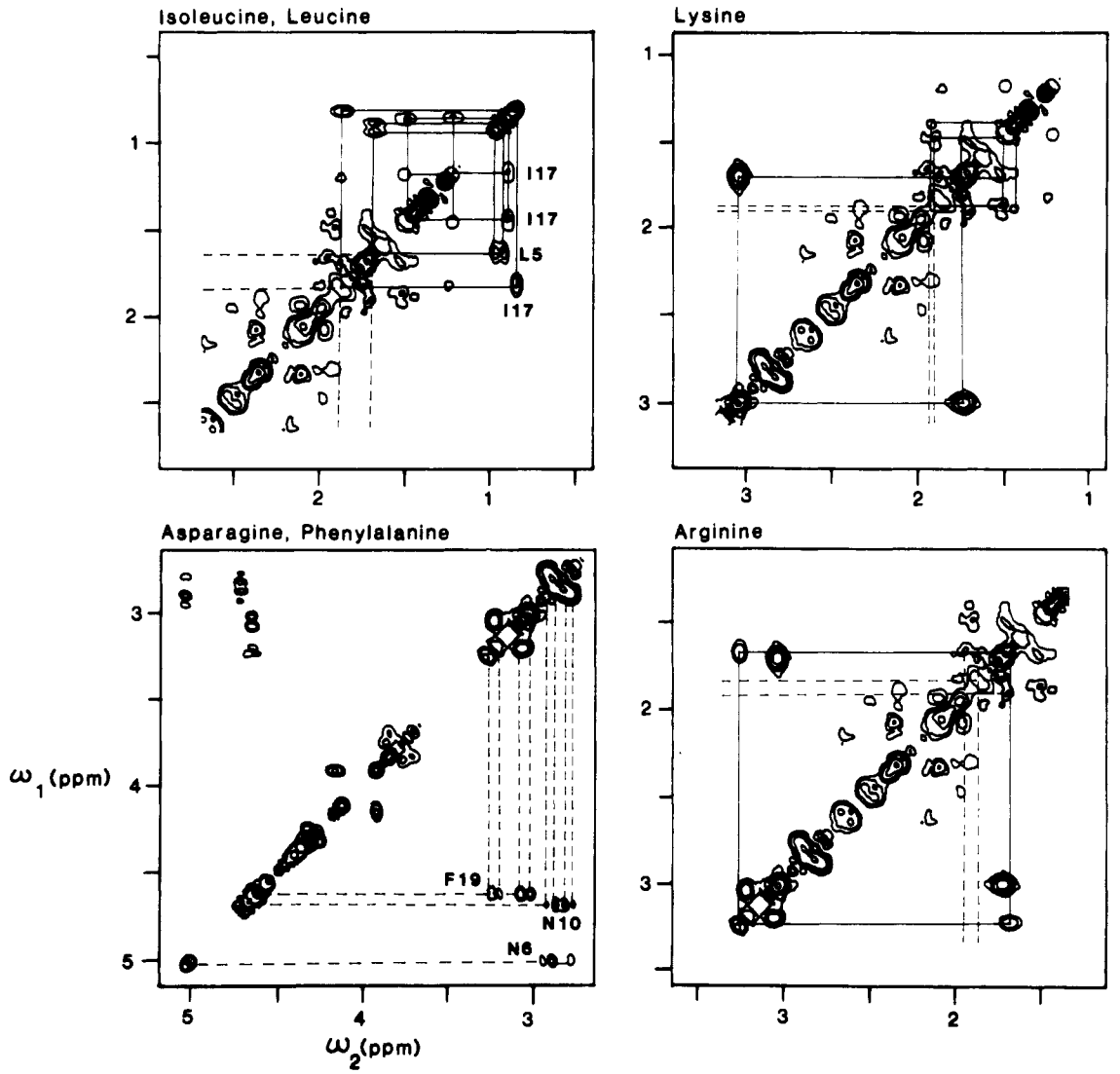

FIGURE 6: Enlarged view of regions of a DQCOSY spectrum obtained at pH 5.0 showing the characteristic correlation patterns for Phe, Ile, Lys, Leu, Asn, and Arg residues.

value in small peptides. The second Thr γCH_3 is moved markedly downfield to 1.316 ppm while its corresponding βCH resonates considerably upfield at 4.135 ppm. Moreover, the αCH in this unusual Thr is shifted nearly 0.5 ppm upfield to 3.883 ppm at pH 5.0 and is pH dependent. On this basis, it is clearly identified as the N-terminal Thr-1 while the normal Thr spin system is due to Thr-15. Moreover, the αCH at 3.883 ppm is coupled to the NH at 8.310 ppm of Glu-2 as described earlier.

(*6*) *Proline.* Both Pro-4 and Pro-7 are responsible for inducing downfield shifts in the residues adjacent to them on their N-terminal sides. The Pro spin systems are more difficult to follow than most others. They consist of two δ, two γ, two β, and one α proton. Table I shows that in small unstructured peptides the δ and γ resonances are each equivalent with chemical shifts of 3.653 and 2.030 ppm, respectively. the βCH_2 chemical shifts are separate and have values of 2.295 and 1.981 ppm, and the αCH resonates at 4.471 ppm. The DQCOSY spectrum in Figure 5 and 1-D spin decouplings at pH 3.0 were used to assign the Pro spin systems. The γCH_2 δ from both Pro residues was found to be 2.032 ppm. Perusal of the 2-D spectrum and systematic decoupling around this δ verified that the δCH_2 resonances form a system with a major resonance at 3.803 ppm and smaller ones at 3.715 and 3.652 ppm. Each of the latter two resonances was from a different Pro residue since they were each coupled to the major resonance at 3.803 ppm. An expanded view of the coupling of the Pro δCH_2 resonances can be seen in Figure 6. Because the two pairs of γCH_2 protons have an identical δ, the spin system of each individual Pro cannot be followed from the DQCOSY data. Two sets of βCH_2 resonances were identified together with the couplings to their δCH resonances. They are 2.041 and 1.886 ppm coupled to 4.634 ppm and 2.296 and 1.868 ppm coupled to 4.415 ppm.

One-dimensional NOED spectra were obtained so as to reveal the βCH_2 resonances arising from the same ring as the given δCH_2 resonances. In this way, the complete spin system of each Pro was obtained. The assignment of a given set of resonances to a particular Pro residue was then made on the basis of NOED connectivities to Ala-3 αCH and to Asn-6 αCH as described earlier. The complete spin systems are shown in Table I. Pro-7 has an αCH which is markedly shifted downfield with respect to the δ in unstructured peptides. This same Pro also displays upfield-shifted βCH_2 resonances. It is therefore likely that Pro-7 is situated in a more structured environment than Pro-4.

Amide Proton Assignments. Having completed all the αCH assignments, the NH resonances remained to be assigned. A spectrum of the amide region of a 3.0 mM solution of the peptide in H_2O is shown in Figure 7. A two-level spin de-

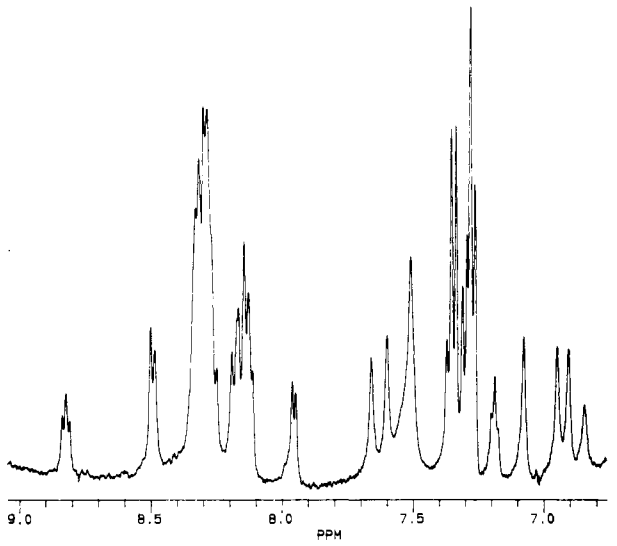

FIGURE 7: Proton NMR spectrum of a 3.0 mM solution of peptide 106–124 in H_2O at pH 5.0 and 298 K showing the amide proton resonances.

Table II: Chemical Shifts of Amide Backbone Proton Resonances in Actin Peptide 106–124 at 298 K, 3.0 mM, and pH 5.0 Together with $^3J_{NHCH}$ Coupling Constants[a]

residue	no.	δ	J (Hz)
Ala	3	8.487 (8.249)	6.0
	9	7.949 (8.249)	5.2
Glu	2	8.310 (8.368)	7.6
	12	8.121 (8.368)	7.2
Phe	19	8.176 (8.228)	6.4
Ile	17	8.121 (8.195)	6.8
Lys	8/13	8.278 (8.408)	5.2
Leu	5	8.114 (8.423)	5.6
Met	14/18	8.317 (8.418)	6.8
Asn	6	8.487 (8.747)	6.0
	10	8.809 (8.747)	5.2
Gln	16	8.823 (8.411)	5.2
Arg	11	8.270 (8.274)	6.0
Thr	15	8.276 (8.236)	6.0

[a] The chemical shifts of the amide protons in unstructured tetrapeptides (from Bundi & Wüthrich, 1979) are shown in parentheses.

coupling technique was used to irradiate the αCH resonances, and the NH resonance collapse was observed in the coupled NH proton. The assignments are listed in Table II together with the $^3J_{CHNH}$ coupling constants and the δ expected from NH resonances in small unstructured peptides, which exhibit coupling constants of 7–7.5 Hz (Bundi & Wüthrich, 1979; Mendz & Moore, 1985). Several of the coupling constants are small, with values as low as 5.2 Hz, indicating that at least some of the backbone of the peptide is significantly constrained. The most unusual amides include Ala-3, Leu-5, Asn-6, Lys-8, Ala-9, Asn-10, Arg-11, Glu-12, Lys-13, Thr-15, and Gln-16 based on measurements of coupling constants and/or the difference in δ from the value in unstructured peptides.

Discussion

The actin peptide 106–124 is clearly involved in binding ATP, and it has a sufficient number of residues on either side of the segment 114–118 to suggest that it is a good model for the corresponding region in actin. Evidence was also presented which showed that tripolyphosphate interacted with the peptide 106–124, but with a lower affinity than ATP since the exchange rate was much faster. Therefore, the triphosphate moiety of ATP appears to be largely responsible for binding to the peptide. Binding of ATP appears to be mainly accomplished through the interaction of the two negatively charged terminal phosphates with the positive side chains of Arg-116 and Lys-118. The adenosine moiety normally interacts with the actin monomer (Mihashi & Wahl, 1975). However, under special circumstances, the adenosine appears to be mobilized (Barden et al., 1980; Curmi et al., 1982) while ATP remains firmly bound via the triphosphate side chain (Barden et al., 1980). The β- and γ-phosphates in particular are involved in binding ATP to actin (Cozzone et al., 1974; Brauer & Sykes, 1981). Thus, the triphosphate appears to be most important in the interaction of ATP with actin and correspondingly with the peptide 106–124.

The synthetic peptide is almost completely insoluble at alkaline pH and has a low solubility in acid conditions, presumably caused by the presence of either or both of the chain extensions to the pentapeptide 114–118. The only positive side chains in the peptide ANREK are Arg-116 and Lys-118. Figures 1 and 2 clearly show that the presence of ATP causes a broadening in some of the Arg and Lys resonances and a shift in others. No significant effects were observed in other residues.

Examination of the effect of tripolyphosphate binding to the peptide (Figure 4) with reference to the completed assignments in Table I reveals that there is a selective broadening of the side-chain resonances. Many of the resonances are readily identifiable. These include the βCH_2 of Gln-16 at 2.438 ppm, which is more than half broadened, the δCH_3 (0.806 ppm) and $\gamma' CH_3$ (0.844 ppm) of Ile-17, which are both more than half broadened, the ϵCH_3 of Met-18 at 2.059 ppm, which is completely broadened, and the aromatic resonances of Phe-19 at 7.290–7.360 ppm, which are also reduced to about half their original intensity. Moreover, the intensities of the Asn-10 βCH_2 resonances at 2.829 and 2.774 ppm are reduced by nearly half, and the βCH_2 of Arg-11 at 3.213 ppm is similarly reduced to about half the original intensity. One of the Lys ϵCH_2 resonances appears to have been completely broadened. It has a δ of 3.003 ppm. The N-terminal seven residues appear unaffected together with a second Lys residue, Ala-9, Glu-12, Met-14, and Thr-15. These observations indicate that Lys-13, as part of the ATP binding sequence 114–118, is probably involved in the binding of tripolyphosphate. Consequently, the ϵCH_2 resonance at 3.003 ppm is assigned to Lys-13, and the ϵCH_2 resonance at 2.992 ppm, which appears to remain unaffected by tripolyphosphate binding, is assigned to Lys-8 (Table I).

Full assignment of all proton resonances in the ATP binding peptide 106–124 has shown that the majority of the residues exist in an ordered environment. The backbone protons in particular exhibit chemical shifts and $^3J_{NHCH}$ coupling constants indicative of a well-ordered structure. The Ala-3 and Asn-6 αCH shifts demonstrate that there are close interactions with the Pro rings, and the δ of some of the Pro resonances indicates that there may be at least one Pro turn.

The typical values of $^3J_{NHCH}$ obtained in unstructured peptides are about 7–7.5 Hz (Mendz & Moore, 1985) so that a value of 6 Hz may indicate some rotational constraint. Values as low as 5.2 Hz, however, are definite indicators of restricted motion unlike that observed in random coils (De Marco et al., 1978). The amide coupling constant of Leu-5 (5.6 Hz) and its δ both show evidence of structure along this segment of the peptide. Indeed, the $^3J_{NHCH}$ values of Lys-8 (5.2 Hz) and Asn-9 (5.2 Hz) indicate that the ordered backbone extends well past Pro-7. Arg-11 does not appear to be in a particularly well-ordered environment on the basis of the δ of its αCH and NH proton resonances, but its $^3J_{NHCH}$

is only 6.0 Hz so it is unlikely to lie in an unordered structure. The δ of the NH of Glu-12 is shifted markedly upfield (0.247 ppm) from its position in small unordered peptides, and Lys-13 also displays evidence of structure with a $^3J_{NHCH}$ of only 5.2 Hz and a downfield shift in the δ of its NH resonance of 0.130 ppm.

Of the sequence extending beyond the C-terminal end of the peptide ANREK, the backbone of Met-14 does not appear to be in a very structured environment although the ϵCH_3 is influenced by some structure, as is the ϵCH_3 of Met-18. The $^3J_{NHCH}$ of Thr-15 (6.0 Hz) provides some evidence of backbone constraint. The environment of Gln-16 is very well-ordered. The δ values of all the side-chain resonances of Gln-16 diverge from the values expected in a random structure. The δ of the NH is shifted upfield by 0.412 ppm, and the $^3J_{NHCH}$ is only 5.2 Hz. The δ of the αCH of Ile-17 is shifted significantly upfield (0.139 ppm), and the other side-chain resonances are also shifted from the position expected in small unordered peptides. Little evidence of structure is obtained from the measurements of the NH δ and $^3J_{NHCH}$ of either Ile-17 or Met-18 except perhaps for a 0.101 ppm upfield shift in the Met-18 NH δ. As mentioned previously, the δ of the ϵCH_3 of Met-18 provides some evidence that the side chain is influenced by some structure. Finally, Phe-19 also displays some evidence of being in a restricted environment even though it is the C-terminal residue. All the side-chain proton resonances differ from their random-coil positions. The βCH_2 resonances are much closer together; the αCH δ is 0.068 ppm upfield, and the NH δ is 0.062 ppm upfield. The $^3J_{NHCH}$ of Phe-19 is a relatively small 6.4 Hz.

The involvement of residues Asn-10 to Lys-13 and the C-terminal tetrapeptide Gln-16 to Phe-19 in the binding of tripolyphosphate indicates that there may be a reverse turn in the C-terminal segment which brings the two segments close together.

Evidence has been presented which shows that the actin sequence 106–124, incorporating 114–118, binds ATP through the triphosphate side chain. The synthetic nonadecapeptide exhibits a well-ordered structure, and as such, an exhaustive structural analysis of the peptide should prove to be a productive endeavor. It is hoped that the identification in this paper of an ATP binding sequence will prove useful for the study of homologous ATP binding regions in other proteins (Walker et al., 1982; Argos & Leberman, 1985).

ACKNOWLEDGMENTS

J.A.B. thanks Dr. G. L. Mendz (Department of Biochemistry, The University of Sydney) for helpful advice on NMR techniques and A/Pro. C. G. dos Remedios for helpful discussions.

Registry No. 5′-ATP, 56-65-5; actin peptide 106–124, 106436-19-5.

REFERENCES

Argos, P., & Leberman, R. (1985) *Eur. J. Biochem. 152*, 651–656.

Asakura, S. (1961) *Arch. Biochem. Biophys. 92*, 140–149.

Barden, J. A., & Miki, M. (1986) *Biochem. Int. 12*, 321–329.

Barden, J. A., Cooke, R., Wright, P. E., & dos Remedios, C. G. (1980) *Biochemistry 19*, 5912–5916.

Barden, J. A., Miki, M., Hambly, B. D., & dos Remedios, C. G. (1986) *Eur. J. Biochem.* (in press).

Brauer, M., & Sykes, B. D. (1981) *Biochemistry 20*, 6767–6775.

Bundi, A., & Wüthrich, K. (1979) *Biopolymers 18*, 285–297.

Cozzone, P. J., Nelson, D. J., & Jardetsky, O. (1974) *Biochem. Biophys. Res. Commun. 60*, 341–347.

Curmi, P. M. G., Barden, J. A., & dos Remedios, C. G. (1982) *Eur. J. Biochem. 122*, 239–244.

De Marco, A., Llinas, M., & Wüthrich, K. (1978) *Biopolymers 17*, 617–636.

dos Remedios, C. G., & Cooke, R. (1984) *Biochim. Biophys. Acta 788*, 193–205.

Grathwohl, C., & Wüthrich, K. (1976a) *Biopolymers 15*, 2025–2042.

Grathwohl, C., & Wüthrich, K. (1976b) *Biopolymers 15*, 2043–2057.

Hegyi, G., Szilagyi, L., & Elzinga, M. (1985) *J. Muscle Res. Cell Motil. 6*, 74.

Hodges, R. S., & Merrifield, R. B. (1975) *Anal. Biochem. 65*, 241–272.

Jacobson, G., & Rosenbusch, J. (1976) *Proc. Natl. Acad. Sci. U.S.A. 73*, 2742–2746.

Jones, C. R., Sikakana, C. T., Hehir, S., Kuo, M.-C., & Gibbons, W. A. (1978) *Biophys. J. 24*, 815–832.

Kabsch, W., Mannherz, H. G., & Suck, D. (1985) *EMBO J. 4*, 2113–2118.

Kemp, B. E. (1979) *J. Biol. Chem. 254*, 2638–2642.

Mendz, G. L., & Moore, W. J. (1985) *Biochem. J. 229*, 305–313.

Mihashi, K., & Wahl, P. (1975) *FEBS Lett. 52*, 8–12.

Miki, M., & Wahl, P. (1984) *Biochim. Biophys. Acta 786*, 188-196.

Miki, M., Barden, J. A., & dos Remedios, C. G. (1986) *Biochim. Biophys. Acta 872*, 76–82.

Piantini, U., Sørensen, O. W., & Ernst, R. R. (1982) *J. Am. Chem. Soc. 104*, 6800–6801.

Rance, M., Sørensen, O. W., Bodenhausen, G., Wagner, G., Ernst, R. R., & Wüthrich, K. (1983) *Biochem. Biophys. Res. Commun. 117*, 479–485.

Shaka, A., & Freeman, R. (1983) *J. Magn. Reson. 51*, 169–173.

Stewart, J. M., & Young, J. P. (1966) *Solid State Peptide Synthesis*, pp 44 and 66, W. H. Freeman, San Francisco, CA.

Vandekerckhove, J., & Weber, K. (1984) *J. Mol. Biol. 179*, 391–413.

Vandekerckhove, J., Deboben, A., Nassal, M., & Wieland, T. (1985) *EMBO J. 4*, 2815–2818.

Walker, J. E., Saraste, M., Runswick, M. J., & Gay, N. J. (1982) *EMBO J. 1*, 945–951.